

# Turnover-based *in vitro* selection and evolution of biocatalysts from a fully synthetic antibody library

Sandro Cesaro-Tadic<sup>1</sup>, Dimitrios Lagos<sup>2,4</sup>, Annemarie Honegger<sup>1</sup>, James H Rickard<sup>3</sup>, Lynda J Partridge<sup>2</sup>, G Michael Blackburn<sup>3</sup> & Andreas Plückthun<sup>1</sup>

This report describes the selection of highly efficient antibody catalysts by combining chemical selection from a synthetic library with directed *in vitro* protein evolution. Evolution started from a naive antibody library displayed on phage made from fully synthetic, antibody-encoding genes (the Human Combinatorial Antibody Library; HuCAL-scFv). HuCAL-scFv was screened by direct selection for catalytic antibodies exhibiting phosphatase turnover. The substrate used was an aryl phosphate, which is spontaneously transformed into an electrophilic trapping reagent after cleavage. Chemical selection identified an efficient biocatalyst that then served as a template for error-prone PCR (epPCR) to generate randomized repertoires that were subjected to further selection cycles. The resulting superior catalysts displayed cumulative mutations throughout the protein sequence; the ten-fold improvement of their catalytic proficiencies ( $>10^{10} \text{ M}^{-1}$ ) resulted from increased  $k_{\text{cat}}$  values, thus demonstrating direct selection for turnover. The strategy described here makes the search for new catalysts independent of the immune system and the antibody framework.

Whereas the improvement of enzymes by molecular engineering increasingly extends their use in biotechnology, the generation of novel protein catalysts remains largely a basic research goal, albeit one with considerable potential once high turnover numbers are achieved<sup>1–4</sup>. Antibodies are considered useful candidates for mimicking the process of divergent protein evolution. The versatile immunoglobulin structure combines stability with diversity, allowing specific, high-affinity binding to virtually any chemical ligand. Somatic hypermutation adds an element of directed evolution, but only for binding affinity. Historically, the availability of natural antibodies as the first protein ‘library’ and the provision by the immune system of a ‘selection technology’ led to the choice of the antibody scaffold for the development of catalysis<sup>5,6</sup>.

Catalytic antibodies (abzymes) have generally been produced by immunization with transition state analogs (TSAs) or ‘bait-and-switch’ haptens to raise antibody binding pockets complementary to an intermediate state of the reaction<sup>5–7</sup>. Although these experiments have facilitated the development of certain general guidelines in hapten design, most attempts have resulted in only moderate proficiencies compared with naturally occurring enzymes. Possible reasons include imperfect hapten features, the use of indirect selection for binding only, the limited size of the natural immune repertoire and, most importantly, the absence of iterative evolution cycles for catalysis. Other approaches using reactive ligands<sup>8–10</sup> and mechanism-based inhibitors<sup>10–15</sup> have been devised to overcome some conceptual limitations. Mechanism-based inhibition involves covalent capture of active catalysts only after turnover of a specified reaction and therefore

a more direct link of the triggering of B cells to catalysis. Nevertheless, screening by the classical immunization protocol remains cumbersome and exerts no pressure on the catalyst to evolve for turnover.

Here we report the direct selection of catalysts from a naive, fully synthetic library and their subjection to directed evolution for improved turnover. The HuCAL-scFv consists of fully synthetic, modular genes optimized for *Escherichia coli* expression<sup>16,17</sup>. The defined library composition and compatible complementarity-determining region (CDR) and framework region modules allow easy manipulation, even with pools of molecules. Most importantly, HuCAL-scFv permits not only an initial selection, but subsequent iterative directed evolution of catalysts, and the approach is independent of the constraints imposed by immunization to generate hapten binders.

A direct screen for catalysis was applied to the HuCAL-scFv library (functional size  $2 \times 10^9$ ) displayed on filamentous phage. Phosphate monoester bond cleavage of the anchored 2-difluoromethylphenyl phosphate (DFMPP) substrate, leading to formation of an anchored quinonemethide and subsequent covalent attachment of active protein species, allowed rapid identification of candidate clones, from which a catalyst (TT1) with good rate enhancement was selected. Second-generation mutated libraries were created from the scFv TT1 template and used to select for improved catalysts. Phenotypes evolved directly for turnover rather than for substrate recognition were selected from the mutated libraries. This approach may lead to new guidelines in generating and evolving tailored enzyme activities and selectivities *in vitro*.

<sup>1</sup>Biochemisches Institut, Universität Zürich, Winterthurerstrasse 190, CH-8057 Zürich, Switzerland. <sup>2</sup>Krebs Institute, Department of Molecular Biology and Biotechnology, University of Sheffield, Western Bank, Sheffield, S10 2TN, UK. <sup>3</sup>Krebs Institute, Department of Chemistry, Sheffield University, Sheffield, S3 7HF, UK. <sup>4</sup>Present address: Wolfson Institute for Biomedical Research, University College London, Gower Street WC1E 6BT, London, UK. Correspondence should be addressed to A.P. (plueckthun@bioc.unizh.ch) or G.M.B. (g.m.blackburn@sheffield.ac.uk).

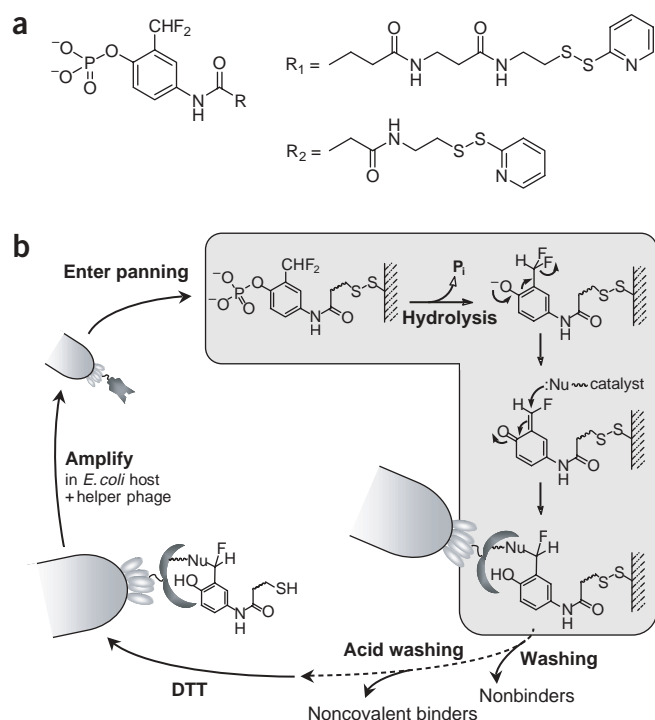


**Figure 1** Capturing phage for catalyst selection with a mechanism-based reaction scheme. **(a)** Structure of difluoromethylphenyl phosphate (DFMPMP). **(b)** DFMPMP, immobilized to BSA or transferrin, was used in turnover selection from the phage-displayed HuCAL-scFv for catalysis of phosphate monoester hydrolysis. This selection approach covers the entire cycle of phosphate monoester hydrolysis and subsequently leads to formation of an electrophilic quinonemethide, which bonds covalently to the protein catalyst and links it to the surface for selection. Nonbinding and noncovalently bound phages were removed by washing with buffer and 0.1 M glycine-HCl, pH 2.2, respectively. The covalently trapped library pools were released by disulfide reduction with dithiothreitol (DTT). Rescued phages were amplified by passage through a bacterial host for subsequent rounds of selection or were subcloned for soluble expression. Because all panning and subsequent screening procedures were conducted in 96-well format, the process allowed rapid identification of candidate clones.

## RESULTS AND DISCUSSION

### Selection chemistry

The reactive DFMPMP (Fig. 1a) was synthesized as a turnover-based substrate trap for covalent capture of catalytic protein<sup>18</sup>. Such substrates act as inhibitors by binding to the active site, where conversion into the reactive species causes covalent modification and irreversible inhibition. For DFMPMP, after catalytic hydrolysis of the phosphate ester, transformation by spontaneous fluoride elimination yields a reactive quinonemethide species. This may trap the protein catalyst by bonding to a nucleophile at or near the active site (Fig. 1b). This process necessarily selects for catalyzed turnover of phosphate ester cleavage. Thus, the specificity and reactivity of the inhibitor is determined by the rates of the individual chemical steps<sup>19,20</sup> but is independent of the mechanism of phosphate ester cleavage<sup>18</sup>. The formation of the reactive quinonemethide from phenol is normally slow<sup>21</sup>, and it is not known whether the protein catalyst actively assists in fluoride elimination<sup>18–20</sup>. The quinonemethide must react with the protein before dissociation from the active site. The desired performance of the immobilized DFMPMP has been demonstrated by trapping of alkaline phosphatase (AP)<sup>18</sup>. Trapping was also shown for an active site AP mutant (S112A),

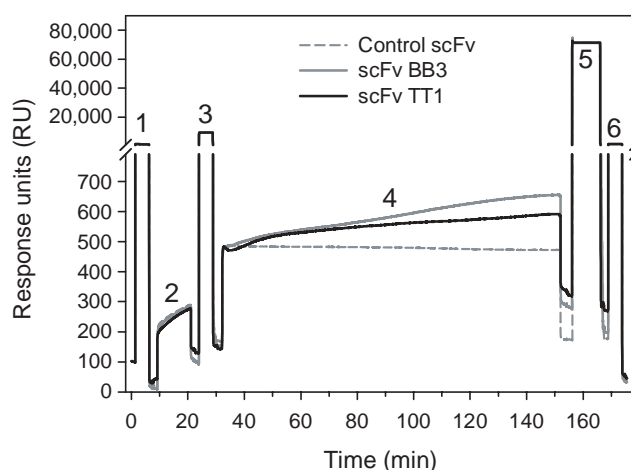


**Figure 2** Catalyst screening for covalent linkage with the turnover-based substrate. The optical biosensor allows sensitive quantification of molecular interactions (in RU) that can be monitored in real time. The substrate DFMPMP was immobilized on the thiol-activated sensor chip (step 1) in a defined orientation by disulfide exchange (step 2). Excess thiol was deactivated (step 3), and scFv antibodies (0.2  $\mu$ M) were injected for 2 h (step 4). Antibody fragments TT1 and BB3 were bound at intensities of 177 RU and 123 RU, respectively. Noncovalently attached protein was washed off with buffer containing 6 M guanidinium chloride (step 5). The remaining signals of 126 RU and 44 RU refer to covalently trapped antibody, which corresponds to 71% and 36% of the entire bound scFv TT1 and scFv BB3, respectively. Unselected scFvs injected as controls and unrelated proteins (e.g. BSA) did not activate the mechanistic trap, nor did they bind at all to the inhibitor<sup>18</sup>. No binding of scFvs to an underivatized surface was observed (not shown). Disulfide bond cleavage finally released the antibody-inhibitor complexes (step 6).

several orders of magnitude less active than wild type enzyme, but still  $10^5$ -fold faster than the uncatalyzed reaction. The system is thus capable of identifying both highly efficient and poorly active catalysts<sup>18</sup>.

### Covalent trapping of phages displaying catalytic scFv fragments

We sought to identify catalysts from the highly diverse HuCAL-scFv library by covalent binding to the trapping reagent (Fig. 1b). The phage library was panned against immobilized BSA and transferrin conjugates of DFMPMP. Nonbinding and noncovalently bound phages were removed by washing with buffer and acid, respectively. Covalently bound phages were released with 10 mM dithiothreitol (DTT) and amplified in *E. coli*. To minimize selection of protein binders, phages were applied alternately to BSA- and transferrin-substrate conjugates in subsequent rounds of panning.

Phage titers resulting from different selection conditions were analyzed. Most phages were removed by the stringent washing conditions of the first selection round, including acid washing, allowing rapid preliminary selection of candidate catalysts. The duration of incubation (1–20 h) with DFMPMP substrate and washing steps did not substantially affect the ratio of input to output phages, presumably because the acid wash removes noncovalent binders. Enrichment factors of 20- to 70-fold per round were observed, indicating selection of covalently attached phages by the turnover-based substrate from very few panning cycles.

After two rounds of panning, DNA from 370 randomly chosen members of the selected polyclonal phage pools was subcloned for soluble periplasmic expression of scFv fragments. Specific binding of the DFMPMP reagent was shown in standard ELISA for most individual

**Table 1** Kinetic properties of TT1 and the two evolved mutants TT1.D1 and TT1.D2

	$k_{\text{cat}}$ ( $\text{s}^{-1}$ )	$k_{\text{cat}}/k_{\text{uncat}}$	$K_{\text{m}}$ ( $\mu\text{M}$ )	$k_{\text{cat}}/K_{\text{m}}$ ( $\text{s}^{-1} \text{M}^{-1}$ )	$(k_{\text{cat}}/K_{\text{m}})/k_{\text{uncat}}$ ( $\text{M}^{-1}$ )
scFv TT1	$5.0 \times 10^{-4}$	$2.3 \times 10^5$	46	10.9	$4.9 \times 10^9$
scFv TT1.D1	$4.9 \times 10^{-3}$	$2.3 \times 10^6$	71	69	$3.1 \times 10^{10}$
scFv TT1.D2	$3.9 \times 10^{-3}$	$1.8 \times 10^6$	31	127	$5.7 \times 10^{10}$
IgG or Fab 38E1	$2.0 \times 10^{-5}$	$9.0 \times 10^3$	155	0.13	$5.9 \times 10^7$
AP ( <i>E. coli</i> )	30	$>10^{10}$	35	$8.6 \times 10^5$	$>10^{14}$

Catalytic parameters were determined from phosphatase activity assays with *p*-NPP at 25 °C as shown in **Figure 5**. Parameters for IgG or Fab 38E1 (ref. 23) were determined at 30 °C in 50 mM CHES (2-(*N*-cyclohexylamino)ethanesulfonic acid), 25 mM NaCl, pH 9.0. For *E. coli* alkaline phosphatase (AP), various  $k_{\text{cat}}/k_{\text{uncat}}$  values ( $10^{10}$ – $10^{15}$ ) were reported<sup>27,28,43,44</sup> at 25 °C in different buffer systems, with different substrates showing great variation in  $k_{\text{uncat}}$ , but much smaller differences in  $k_{\text{cat}}$ .

clones and confirmed in competitive-inhibition ELISA for positive clones; half-maximal inhibition occurred at inhibitor concentrations ranging from  $10^{-2}$  to  $10^{-6}$  M.

Binding of candidate scFvs to the reactive substrate was also analyzed by BIAcore<sup>18</sup>. Monitored in real time, covalent binding is indicated by very slow association to the chip, because only a fraction of the molecules are trapped after turnover. Covalently trapped molecules remain bound after washing with 6 M guanidinium chloride (GdmCl). Of six scFv fragments initially analyzed, two (TT1 and BB3) exhibited slow, progressive binding to the anchored DFMP substrate upon prolonged exposure (**Fig. 2**), similar to AP<sup>18</sup>. After extensive washing with GdmCl, >70% and 30% of the scFvs TT1 and BB3, respectively, remained bound. Nonspecific binding to the substrate by other unselected antibody fragments or by BSA was not observed. These findings are consistent with covalent trapping of the scFv fragments by the turnover-based inhibitor.

### Identification and characterization of scFv TT1 as a catalyst

To examine their phospho-monoesterase activity, the selected scFvs were purified by affinity, ion exchange and gel filtration chromatography as native monomeric proteins (>95% purity on SDS-PAGE). Care was taken to exclude possible traces of contaminating enzymes. ScFv protein purified under native conditions retained equivalent specific activities in repeated preparations. Also, purified His-tagged protein was reloaded onto a nickel ion affinity column and denatured with 6 M GdmCl to remove potentially tightly bound contaminants. After renaturation on the column, the specific activity of the scFv was maintained. Furthermore, scFvs refolded from inclusion bodies and purified by immobilized metal ion affinity (IMAC) and ion exchange chromatography showed similar specific activities. Other antibody fragments purified under the same conditions did not show catalytic activity. Finally, mutations in the scFv (see later) abolished phosphatase activity.

Phosphatase activity was measured using *p*-nitrophenyl phosphate (*p*-NPP) as the substrate and monitoring release of *p*-nitrophenol spectrophotometrically at 405 nm. Antibody TT1 showed greatest activity and was characterized in more detail. The rate enhancement above background ( $k_{\text{cat}}/k_{\text{uncat}}$ ) was found to be  $2.3 \times 10^5$ ; TT1 catalyzed phosphate hydrolysis with  $k_{\text{cat}} = 0.03 \text{ min}^{-1}$  and  $K_{\text{m}} = 46 \mu\text{M}$ , corresponding to a second-order rate constant ( $k_{\text{cat}}/K_{\text{m}}$ ) of  $10.9 \text{ s}^{-1} \text{M}^{-1}$  and a catalytic proficiency ( $k_{\text{cat}}/k_{\text{uncat}}/K_{\text{m}}$ ) of  $5 \times 10^9 \text{ M}^{-1}$ .

At this point only a few abzymes for phosphate ester hydrolysis are available; all have only modest performance and were produced by

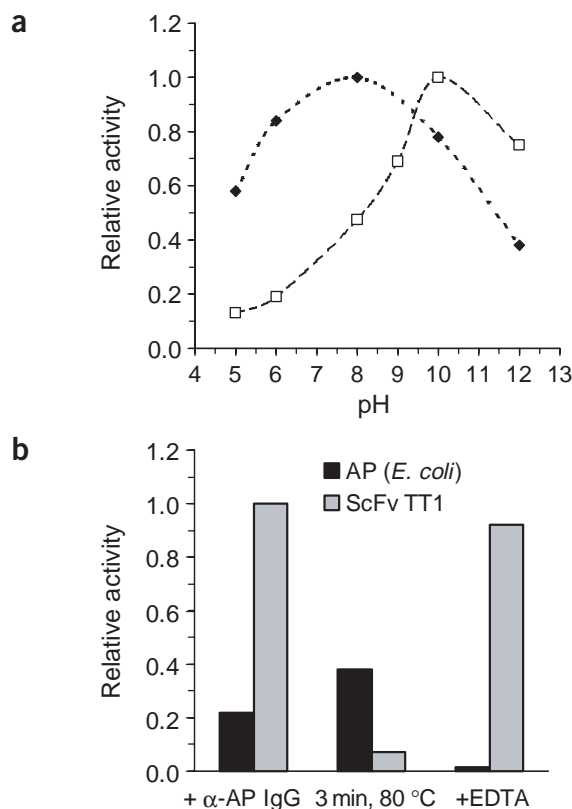


**Figure 3** Catalytic properties of scFv TT1 compared to alkaline phosphatase (AP). (a) The pH versus activity profiles for wild type *E. coli* AP (□) (Calbiochem,  $10^{-5}$  U/well) and purified antibody TT1 (◆) (2  $\mu\text{M}$ ) were determined with 5 mM *p*-NPP at the appropriate buffer conditions (0.1 M MES, pH 5.0–6.5, 0.1 M Tris, pH 7.0–9.0 and CAPS buffer pH 9.5–12; ionic strength adjusted to 0.3 M with NaCl). (b) Influence of different additions on AP and scFv TT1. Activity in assay buffer alone was defined as 1.0 in the determination of relative activities. Activities were measured after addition of α-AP IgG (3 nM IgG directed against AP (*E. coli*); Rockland) or EDTA (5 mM) after preincubation for 30 min; or after preincubation at 80 °C for 3 min. Activity was assayed using 5 mM *p*-NPP in 0.1 M HEPES buffer, pH 8.0, 150 mM NaCl, 1 mM  $\text{MgCl}_2$ .

conventional immunization<sup>5,22</sup>. The first and still the best phosphatase-like antibody<sup>23</sup> displayed phospho-monoesterase activity with  $k_{\text{cat}} = 0.0012 \text{ min}^{-1}$  and  $K_{\text{m}} = 155 \mu\text{M}$ , giving a rate enhancement ( $k_{\text{cat}}/k_{\text{uncat}}$ ) of  $8.0 \times 10^3$  and a catalytic proficiency ( $k_{\text{cat}}/k_{\text{uncat}}/K_{\text{m}}$ ) of  $5.2 \times 10^7 \text{ M}^{-1}$ . Antibody-catalyzed phosphodiester hydrolysis has been described<sup>24,25</sup> with a rate enhancement ( $k_{\text{cat}}/k_{\text{uncat}}$ ) of  $1.7 \times 10^3$  and catalytic proficiency of  $1.7 \times 10^7 \text{ M}^{-1}$ . Catalysts for hydrolysis of phosphate triesters<sup>22,25,26</sup> gave rate enhancements between  $10^2$  and  $10^3$  and catalytic proficiencies in the range of  $10^4$  to  $10^5 \text{ M}^{-1}$ . Overall, the generation of antibody catalysts with phosphoesterase-like activities has been hampered by the lack of suitable trigonal bipyramidal analogs of transition states and by the limited sensitivity of product detection for non-aryl phosphates. Pentavalent coordination spheres, though available in vanadate, are difficult to obtain as stable acyclic compounds that can be linked to a carrier, and vanadates are generally too toxic to be used for immunization, whereas alternative compounds such as rhenium are difficult to obtain in stable acyclic systems<sup>5–7</sup>. Our approach of direct turnover-based selection from an unbiased, fully synthetic protein library circumvents these limitations. The catalytic properties of scFv TT1 are two orders of magnitude

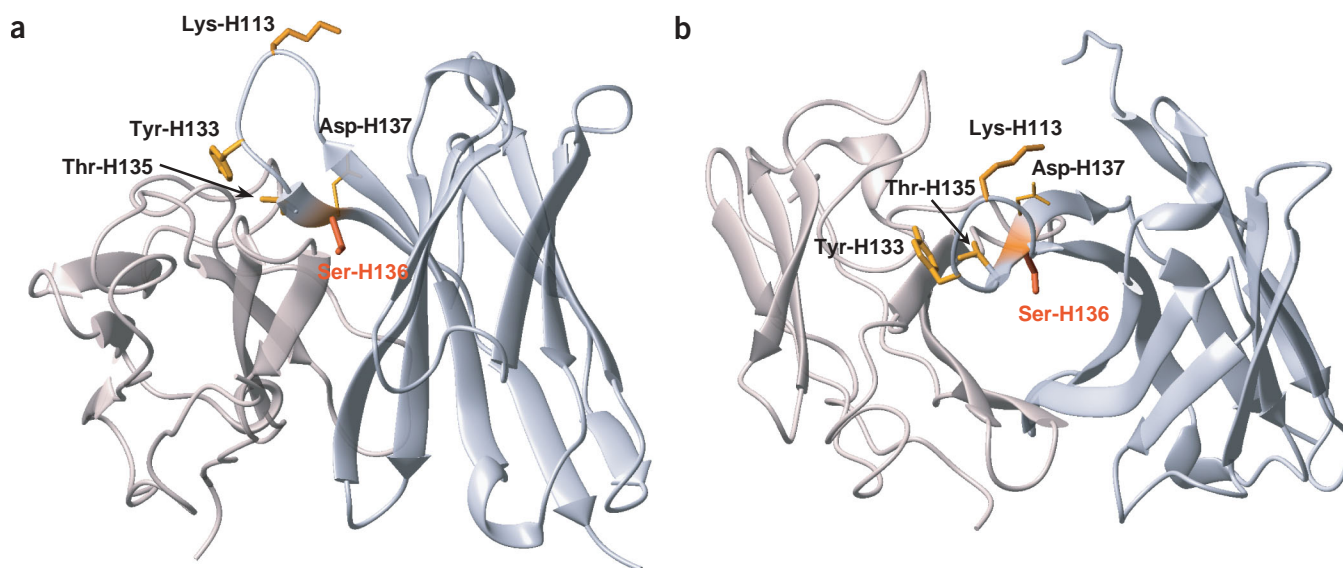


**Figure 4** Three-dimensional homology model structure of scFv antibody fragment TT1. **(a)** Front view and **(b)** top view ribbon presentations. The heavy chain (light blue) and light chain (gray) variable domains refer to the HuCAL-scFv consensus frameworks  $V_H1A$  and  $V_L2$  (Fig. 5c)<sup>16</sup>. Amino acid residues in CDR-H3 that were exchanged to alanine (see text) are shown in orange (Lys-H113, Tyr-H133, Thr-H135, Asp-H137) and red (Ser-H136). The model of the TT1 scFv was based on the HuCAL-scFv VH1A (PDB accession no. 1DHA) and VL2 (PDB accession no. 1DH8) domain models<sup>16</sup>. The CDR-L3 conformation and relative domain orientation was taken from human IgM rheumatoid factor Fab (PDB accession no. 1ADQ), the CDR-H3 conformation from Fab 36-71 (PDB accession no. 6FAB). Numbering is according to Honegger<sup>45</sup>.

superior to the best antibody reported so far for phosphate ester hydrolysis (Table 1). Hence, direct selection rather than TSA binding may prove a more useful and widely applicable approach to generating active catalysts.

The catalytic properties of TT1 were compared to those of AP, the most abundant phosphatase in *E. coli*, which occurs in the periplasmic space (Fig. 3)<sup>27,28</sup>. ScFv TT1 exhibited maximal activity at a pH between 7.5 and 8, and retained activity over a broad pH range (Fig. 3a). Its pH-rate profile differed significantly from that of AP. Incubation with antibodies specific for AP diminished activity of AP by ~80% but had no effect on TT1 activity (Fig. 3b). The scFv was deactivated by heating at 80 °C for 3 min, whereas the bacterial enzyme, known to be stable to heat treatment<sup>28</sup>, retained 40% of its activity. Furthermore, incubation with up to 5 mM EDTA, a chelator of the bivalent metal ions often used by natural phosphatases<sup>28,29</sup>, had no effect on scFv TT1 activity. Vanadate, generally a good mimic of the transition state geometry in phosphate ester hydrolysis, was also found to competitively inhibit the TT1-catalyzed *p*-NPP hydrolysis with a  $K_i$  of 1  $\mu$ M (data not shown).

### Probing the active site by mutation

To investigate the role of specific amino acid residues<sup>30</sup> in TT1 catalysis, ionizable or nucleophilic residues were replaced by alanine. We primarily focused on CDR3 residues of the heavy chain for several reasons. First, CDR mutagenesis is least likely to alter the conformation of the antibody fold. Second, HuCAL-scFv is built using seven  $V_H$  and seven  $V_L$  antibody framework regions with randomized CDR-H3 and CDR-L3 modules<sup>16</sup>. Therefore, it is probable that catalysis is mediated by particular CDR3 loop sequences. Finally, in contrast to the large contact area between antibody CDRs and protein antigens, the contact sites for small haptens are usually close to the pseudo two-fold axis of the Fv fragment and include several framework residues with CDR contributions from both CDR3s<sup>6,31</sup>.

Five amino acids in CDR-H3 (Figs. 4, 5a) were individually exchanged for alanine. Despite slight differences in expression levels, the purified mutated proteins had essentially the same biophysical characteristics. Simultaneous exchange of all five amino acids (Lys-H113, Tyr-H133, Thr-H135, Ser-H136 and Asp-H137; Fig. 5a) rendered the protein catalytically inactive. Single alanine mutations of the residues Lys-H113, Tyr-H133 and Asp-H137 altered the kinetics only slightly (Fig. 5a). In contrast, mutation of the potentially nucleophilic residues Thr-H135 and Ser-H136 severely impaired catalysis. The activity of the T135A mutant was ~15% of that of the parent TT1 scFv, whereas the S136A mutant was essentially inactive. The modified kinetic properties of these mutants correlate well with the homology-modeled structure of scFv TT1 (Fig. 4). Residues Lys-H113, Tyr-H133 and Asp-H137 are loop positions facing the solvent and are thus not likely to be part of an active site pocket. By contrast, Thr-H135 and especially Ser-H136 are buried, facing the putative binding pocket near the pseudo two-fold axis at the  $V_H$ - $V_L$  interface. This region favors the binding of hydrophobic haptens, such as *p*-NPP, in noncatalytic and catalytic antibodies<sup>6</sup> (A.H., unpublished data). The role of Ser-H136, whether in substrate binding, involvement in the  $V_H$ - $V_L$  interface, or even as a catalytic nucleophile, requires further investigation.

### Directed evolution of TT1 for improved turnover

It is thought that enzyme catalytic activity is improved by the iterative randomization and selection inherent in evolution. To mimic the natural selection of enzymes with increased efficiency *in vitro*, directed evolution<sup>1,2</sup> was applied to TT1. In the absence of a crystal structure for the antibody-substrate complex, the whole molecule was randomized by epPCR using nucleoside analogs<sup>32</sup>. This targeted not only the CDRs but also framework regions, with the potential to affect the general scFv conformation and antigen binding site.

The number of mutations per gene can be controlled in epPCR by adjusting the concentration of dNTP analogs. Randomized phage



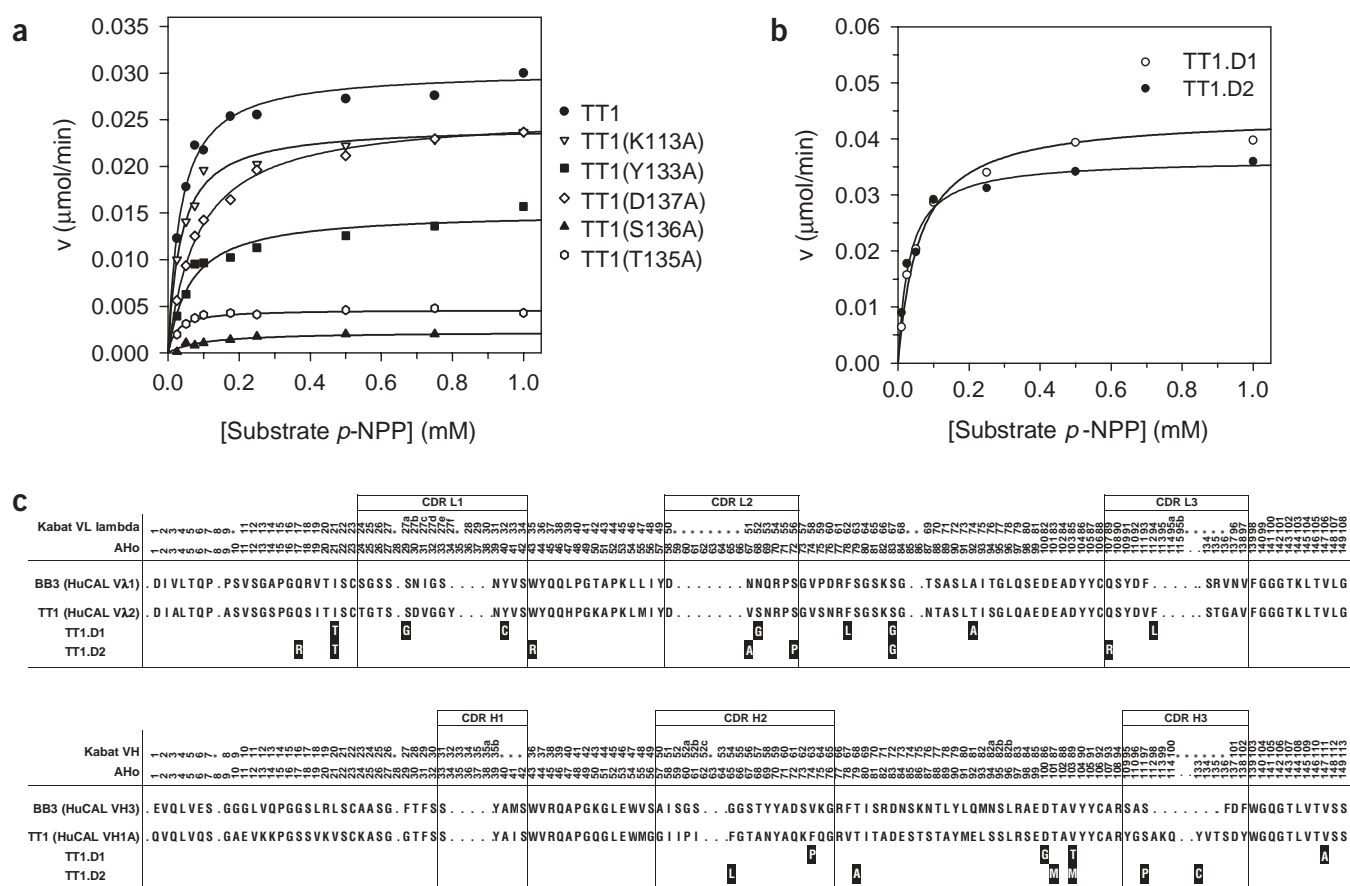


**Figure 5** Catalytic properties of TT1 mutants. **(a)** Effect of single alanine mutations within CDR-H3 of scFv TT1. Phosphatase activities of purified TT1 and five mutants ( $1 \mu\text{M}$  respectively) were assayed with *p*-NPP, and kinetic parameters were fitted to Michaelis-Menten kinetics. TT1 wild type:  $k_{\text{cat}} = 0.03 \text{ min}^{-1}$ ,  $K_m = 46 \mu\text{M}$ ; TT1(K113A):  $k_{\text{cat}} = 0.024 \text{ min}^{-1}$ ,  $K_m = 36 \mu\text{M}$ ; TT1(Y133A):  $k_{\text{cat}} = 0.015 \text{ min}^{-1}$ ,  $K_m = 64 \mu\text{M}$ ; TT1(T135A):  $k_{\text{cat}} = 0.004 \text{ min}^{-1}$ ,  $K_m = 24 \mu\text{M}$ ; TT1(D137A):  $k_{\text{cat}} = 0.026 \text{ min}^{-1}$ ,  $K_m = 85 \mu\text{M}$ ; antibody TT1(S136A) was not subjected to detailed kinetic analysis because of its low activity. **(b)** Catalytic rates of the evolved variants TT1.D1 and TT1.D2. Kinetic parameters were determined as in **a** but with  $0.15 \mu\text{M}$  antibody, respectively (Table 1). As with scFv TT1, >15 turnovers per molecule were measured with no apparent change in  $v_{\text{max}}$ , demonstrating that the antibodies act catalytically. **(c)** Alignment of the amino acid sequences of  $V_H$  and  $V_L$  of selected and evolved scFvs. The HuCAL-scFv frameworks and CDR regions are indicated for the initially selected antibodies TT1 and BB3. For the evolved and selected variants TT1.D1 and TT1.D2, the amino acid mutations are labeled white on black as compared to their progenitor TT1. Additional mutations (one in TT1.D1 and three in TT1.D2) were found in the  $(G_4S)_4$  linker. Numbering of amino acid residues in  $V_H$  and  $V_L$  and the labeling of CDRs is according to Honegger<sup>45</sup> and Kabat<sup>46</sup>.

libraries were constructed with expected mutations of approximately 5 bases per gene (medium) and 15 bases per gene (high). A control library was generated by normal PCR amplification of the TT1 template using a low-fidelity polymerase. The observed error rate for this library was 0.25 mutations per gene, and that of the two epPCR-randomized libraries as predicted. The vast majority of base mutations were transitions (84 and 93% for the medium- and for the high-mutation libraries, respectively)<sup>32</sup>.

The two mutated phage libraries ( $10^5$  clones) and the control library were panned against DFMP. After three rounds, considerable enrichment of eluted phages was observed. The parent TT1 sequence was recovered in 60% of selected clones from the control library and in 10% of clones from the randomized libraries. Sequence analysis of the other selected clones showed that different scFv regions showed mutations after selection; CDR-H1 and CDR-H3 were mutated less and CDR-L2 mutated more in the selected antibodies (data not shown).

Of 10 clones analyzed from the high error rate library, two sequences, TT1.D1 (with 13 mutations) and TT1.D2 (with 16 mutations),

appeared three times and twice, respectively. Both scFvs were expressed, purified and assayed as described earlier, and found to catalyze the hydrolysis of *p*-NPP with Michaelis-Menten kinetics (Fig. 5b). TT1.D1 and TT1.D2 exhibited 7- to 11-fold improved  $k_{\text{cat}}/K_m$  values and catalytic proficiencies, respectively (Table 1), relative to the parent TT1. The improved efficiencies largely result from increased  $k_{\text{cat}}$  values, because the  $K_m$  values of both clones are similar to TT1 (Table 1). The directed evolution thus seems to have responded to selection for turnover rather than for substrate specificity. Cumulative mutations throughout the TT1.D1 and TT1.D2 proteins may contribute to improved catalysis (Fig. 5c) through minor changes in molecule geometry.

#### Evaluation of the strategy

The directed evolution of proteins using libraries generated by high error rate epPCR is generally thought to be not productive because of the very low fraction of functional molecules and the limits imposed on sampling potentially large libraries by the efficiency of *E. coli*

transformation. There is also a popular concept that natural evolution has happened in small, sequential steps<sup>1,33</sup>. However, there now exist several examples of successful directed evolution from such libraries<sup>34–37</sup>, including the affinity maturation of an scFv<sup>38</sup>. The first *in vitro* evolution of a catalytic antibody obtained by classical immunization was described by Fujii and coworkers<sup>39</sup>, who carried out limited randomization of key residues. However, rational library design requires extensive knowledge of structure and function, limits the sequence space searched for increased activity and excludes to a great extent beneficial random changes, notably in the second sphere, that may occur in natural evolution<sup>1</sup>.

By contrast, the selection process used here mimics the principles of natural evolution and extends the means of catalyst selection in two important ways. First, direct selection for turnover is possible even in the absence of tight binding. Second, directed molecular evolution (an iteration of random mutagenesis and selection for turnover) allows improvement of the catalyst. For the monophosphatase described here, this has resulted in 10<sup>3</sup>-fold higher  $k_{\text{cat}}/K_m$  values than those achieved with hybridoma technology<sup>23</sup>. Such selection strategies should be generally applicable for the creation of custom protein catalysts from designed libraries not only of antibodies, but of many other appropriate natural and synthetic scaffolds<sup>40,41</sup>.

## METHODS

**Inhibitor conjugation.** The trapping substrate, a 4-linked-2-difluoromethylphenyl phosphate (DFMPP; Fig. 1a), was synthesized as described<sup>18</sup>. Its pyridyl-2'-disulfide moiety permits coupling to the surface of a sulfhydryl-containing carrier (protein or solid support). Coupling to BSA (Sigma) was as described<sup>18</sup>. BSA conjugates contained an average of four DFMPP molecules, as determined by MS and nonreducing PAGE. Transferrin (Serva) was denatured in 0.2 M Tris buffer, pH 8.6, 8 M urea, and reduced with 100-fold molar excess DTT. After precipitation with 5% trichloroacetic acid (TCA), the pellet was washed twice with 5% TCA, twice with water and dissolved in 50 mM sodium phosphate buffer, pH 7.0, 8 M urea. The free sulfhydryl content of the protein was determined with Ellmann's reagent (Pierce), and disulfide exchange was undertaken immediately with a 10-fold molar excess of DFMPP. Transferrin conjugates contained an average of 25 DFMPP molecules (determined by nonreducing PAGE and MS). The conjugate was dialyzed against 10 mM HEPES, pH 7.5, 150 mM NaCl, 1 mM MgCl<sub>2</sub> and stored at –20 °C.

The accessibility of DFMPP in BSA and transferrin conjugates for dephosphorylation was determined with AP as described<sup>18</sup>.

**Phage library preparation and solid-phase panning.** The phagemid vector pMorph7 was used for phage display and panning procedures<sup>16</sup>. Amplification and purification of HuCAL-scFv phages and phage propagation between two panning rounds were as described<sup>17</sup>. MaxiSorp microtiter plates (Nunc) were coated overnight at 4 °C with 20 µg/well DFMPP-BSA or DFMPP-transferrin. After blocking with 2% (w/v) transferrin, 2% BSA, 5% nonfat dried milk, 0.1% Tween 20 in HBS, 1 × 10<sup>12</sup> to 5 × 10<sup>12</sup> HuCAL-scFv phages were added for variable time periods (1 h to overnight) at 37 °C. Wells were rinsed five times with 0.1% Tween-20 in HBS, five times with HBS and finally with 0.1 M glycine-HCl, pH 2.2, for 10 min at 25 °C. Covalently trapped phages were released by two incubations with 200 µl/well 10 mM DTT in HBS lasting for 15 min each. Eluted phages were used directly to infect 4 ml *E. coli* TG1 culture at a cell density giving an OD<sub>600nm</sub> value of 0.7. Two to three rounds of panning were routinely carried out. Subcloning of DNA from the final selection rounds into the plasmid pMorph7-FH, soluble periplasmic expression under the control of the *lac* promoter in *E. coli* strain JM83 and scFv protein evaluation by ELISA were carried out as described<sup>17</sup>.

**BIAcore screening for covalent capture of selected antibody fragments.** His-tagged scFvs from plasmid pMorph7-FH were expressed in 10 ml bacterial cultures as described<sup>17</sup>. Cells were harvested, resuspended in lysis buffer (50 mM Tris buffer, pH 7.5, 500 mM NaCl, 1 mM MgCl<sub>2</sub>, containing DNase I), disrupted by French press lysis and centrifuged (30 min, 20,000g, 4 °C).

Nickel-nitrilotriacetic acid Superflow (1 ml; Qiagen) was loaded with supernate, washed with 15 ml lysis buffer and then 5 ml lysis buffer containing 10% glycerol and 20 mM imidazole, and eluted in 250 mM imidazole. The eluate was subjected to buffer exchange with 10 mM HEPES, pH 7.5, 150 mM NaCl, 1 mM MgCl<sub>2</sub> by repeated concentration and dilution in a Centricon-10 tube (Millipore). Protein solutions were filtered through a 0.2-µm filter.

All measurements were done using a BIAcore 3000 (BIAcore) equipped with a carboxymethyl-dextran-modified (CM5) sensor chip at a flow rate of 5 µl/min at 20 °C. DFMP ( >95% pure based on MS and NMR) was immobilized directly to the dextran using standard thiol coupling chemistry as described<sup>18</sup>, according to the manufacturer's recommendations. Affinity-purified scFv or periplasmic *E. coli* extracts containing overexpressed proteins were injected into the flow cells for varying times. Noncovalently bound protein was washed off with 6 M GdmCl for 10 min. Finally, disulfide bond cleavage with 0.1 M DTT for 7 min released the scFv-inhibitor complexes.

**Large-scale preparation of scFv antibody fragments.** ScFvs were produced from pMorph7-FH as described earlier but in 2-liter bacterial cultures. At a cell density producing an OD<sub>600nm</sub> of 5, bacteria were pelleted, resuspended in lysis buffer and disrupted by French press lysis. Cell debris was removed by centrifugation and the cleared supernatants filtered through a 0.2-µm membrane. Purifications were done on a BioCAD perfusion chromatography workstation (Applied Biosystems). Supernatants were loaded on an IMAC column with Ni<sup>2+</sup> ions. The column was washed with 20 mM Tris buffer, pH 8.5, 150 mM NaCl, 40 mM imidazole, and His-tag-bound protein was eluted with 250 mM imidazole. Alternatively, the column was washed with buffer and then 6 M GdmCl, after which denaturant was completely removed by extensive washing with buffer and the proteins eluted. Eluates were directly loaded onto a HQ anion exchange column. The column was washed with 20 mM Tris buffer, pH 8.5, 150 mM NaCl, and bound protein was eluted with a NaCl gradient (150–750 mM). Fractions containing scFv (determined by protein immunoblot) were analyzed by Superdex-75 gel filtration on a SMART workstation (Amersham Pharmacia). Fractions containing monomeric scFv were pooled and the buffer exchanged by dialysis against 10 mM HEPES, pH 8.0, 150 mM NaCl, 1 mM MgCl<sub>2</sub>, and repeated concentration and dilution in Centricon-10 tubes. Samples were stored at –80 °C.

For cytoplasmic expression, scFvs were cloned in the vector pTFT74, expressed as inclusion bodies and refolded as described<sup>42</sup>. Refolded His-tagged scFvs were purified by IMAC using Ni-NTA Superflow (Qiagen). The eluate was dialyzed against 20 mM Tris buffer, pH 8.5, 150 mM NaCl and further purified by HQ ion exchange as above.

**Catalytic assay.** Proteins were assayed for phosphatase activity using *p*-NPP as substrate in 0.1 M HEPES, pH 8.0, 150 mM NaCl, 10 mM MgCl<sub>2</sub> at 25 °C. *p*-Nitrophenol formation was monitored spectrophotometrically at 405 nm ( $\epsilon = 18,500 \text{ cm}^{-1} \text{ M}^{-1}$  at pH 8.0) at substrate concentrations of 10 µM–2 mM. The substrate stock solution was usually diluted 20-fold into the antibody solution (0.1–2 µM) to initiate the reaction. The hydrolysis was continued to allow multiple turnovers per antibody molecule. All assays were done at least in triplicate. Kinetic data were fitted to Michaelis-Menten kinetics with SigmaPlot (SPSS Science). The observed first-order rate constant for the uncatalyzed background hydrolysis ( $k_{\text{obs}}$ ) was determined to be  $2.2 \times 10^{-9} \text{ s}^{-1}$  at pH 8.0, 25 °C. All measurements were done in microtiter plates (Nunc) using a Bioassay plate reader (Perkin-Elmer).

**Library generation by epPCR.** To control the number of mutations per gene, randomized phage libraries were generated by epPCR<sup>32</sup> amplification of the TTI template. The gene was amplified from the vector pMorph7-FH with the primers sflacP1 (5'-GTGGAATTGTGAGCG-3') and HuCALrev (5'-TTTTTCACTTCACAG GTC-3'). For epPCR the fragment was amplified using standard conditions, except that 6-(2-deoxy-β-D-ribofuranosyl)-3,4-dihydro-8H-pyrimidino-[4,5-c][1,2]oxazin-7-one-triphosphate (dPTP) and 8-oxo-2'-deoxyguanosine (8-oxo-dGTP) (Amersham Pharmacia) were added. Two libraries were designed with respect to the expected mutation load of 5 and 15 mutations per molecule. Based on 20 PCR cycles the nucleotide analogs<sup>32</sup> dPTP and 8-oxo-dGTP were added at one-fifth (40 µM) and three-fifths (120 µM) of the concentration of each dNTP (200 µM) for the medium- and

high-error library, respectively. The resulting PCR products were separated on a 1.5% agarose gel and purified by gel extraction (Qiagen). The products were cut with *Kpn2I*-*EcoRI* and gel purified. The fragments were ligated into the *Kpn2I*-*EcoRI* digested and gel-purified vector pMorphx7-FH. The library fragments were excised from the plasmid pMorphx7-FH with *XbaI*-*EcoRI* and ligated with phagemid vector pMorph7 that had been cut with *XbaI*-*EcoRI* for use in phage display and panning procedures. The average number of base mutations/amino acid mutations per gene were  $6.9 \pm 2.8/6.1 \pm 2.6$  for library 1 and  $14.8 \pm 5.6/14.0 \pm 5.1$  for library 2.

#### ACKNOWLEDGMENTS

S.C.-T. and D.L. were supported by Studentships under the European Commission Training and Mobility of Researchers program (grant ERBFMRXCT 980193). J.R. was supported by a Biotechnology and Biological Sciences Research Council Studentship. We are grateful to Aziz Mekhalifa and Jason Betley for assistance with chemical synthesis. We are indebted to Bernhard Schimmele, Lutz Jermutus, Stephen Marino and Patrik Forrer for help, advice and discussion, and to MorphoSys AG for the constructive collaboration on HuCAL-scFv.

#### COMPETING INTERESTS STATEMENT

The authors declare competing financial interests (see the *Nature Biotechnology* website for details).

Received 19 November 2002; accepted 21 February 2003

Published online 18 May 2003; doi:10.1038/nbt828

- Schmidt-Dannert, C. Directed evolution of single proteins, metabolic pathways, and viruses. *Biochemistry* **40**, 13125–13136 (2001).
- Farinas, E.T., Bulter, T. & Arnold, F.H. Directed enzyme evolution. *Curr. Opin. Biotechnol.* **12**, 545–551 (2001).
- Griffiths, A.D. & Tawfik, D.S. Man-made enzymes—from design to *in vitro* compartmentalisation. *Curr. Opin. Biotechnol.* **11**, 338–353 (2000).
- Kazlauskas, R.J. Molecular modeling and biocatalysis: explanations, predictions, limitations, and opportunities. *Curr. Opin. Chem. Biol.* **4**, 81–88 (2000).
- Blackburn, G.M., Datta, A., Denham, H. & Wentworth, P. Jr. Catalytic antibodies. *Adv. Phys. Org. Chem.* **31**, 249–392 (1998).
- Hilvert, D. Critical analysis of antibody catalysis. *Annu. Rev. Biochem.* **69**, 751–793 (2000).
- Wentworth, P. Jr. & Janda, K.D. Catalytic antibodies: structure and function. *Cell Biochem. Biophys.* **35**, 63–87 (2001).
- Wirsching, P., Ashley, J.A., Lo, C.H., Janda, K.D. & Lerner, R.A. Reactive immunization. *Science* **270**, 1775–1782 (1995).
- Barbas, C.F., et al. Immune versus natural selection: antibody aldolases with enzymic rates but broader scope. *Science* **278**, 2085–2092 (1997).
- Gao, C., et al. Making chemistry selectable by linking it to infectivity. *Proc. Natl. Acad. Sci. USA* **94**, 11777–11782 (1997).
- Amstutz, P., et al. *In vitro* selection for catalytic activity with ribosome display. *J. Am. Chem. Soc.* **124**, 9396–9403 (2002).
- Janda, K.D., et al. Chemical selection for catalysis in combinatorial antibody libraries. *Science* **275**, 945–948 (1997).
- Soumillion, P., et al. Phage display of enzymes and *in vitro* selection for catalytic activity. *Appl. Biochem. Biotechnol.* **47**, 175–190 (1994).
- Tanaka, F., Lerner, R.A. & Barbas, C.F. Reconstructing aldolase antibodies to alter their substrate specificity and turnover. *J. Am. Chem. Soc.* **122**, 4835–4836 (2000).
- Danielsen, S., et al. *In vitro* selection of enzymatically active lipase variants from phage libraries using a mechanism-based inhibitor. *Gene* **272**, 267–274 (2001).
- Knappik, A., et al. Fully synthetic Human Combinatorial Antibody Libraries (HuCAL) based on modular consensus frameworks and CDRs randomized with trinucleotides. *J. Mol. Biol.* **296**, 57–86 (2000).
- Krebs, B., et al. High-throughput generation and engineering of recombinant human antibodies. *J. Immunol. Methods* **254**, 67–84 (2001).
- Betley, J.R., et al. Direct screening for phosphatase activity by turnover-based capture of protein catalysts. *Angew. Chem., Int. Edn. Engl.* **41**, 775–777 (2002).
- Myers, J.K., Cohen, J.D. & Widlanski, T.S. Substituent effects on the mechanism-based inactivation of prostatic acid phosphatase. *J. Am. Chem. Soc.* **117**, 11049–11054 (1995).
- Born, T.L., Myers, J.K., Widlanski, T.S. & Rusnak, F. 4-(Fluoromethyl)phenyl phosphate acts as a mechanism-based inhibitor of calcineurin. *J. Biol. Chem.* **270**, 25651–25655 (1995).
- Loubinoux, B., Miazimbakana, J. & Gerardin, P. Reactivity of new precursors of quinone methides. *Tetrahedron Lett.* **30**, 1939–1942 (1989).
- Vayron, P., et al. Toward antibody-catalyzed hydrolysis of organophosphorus poisons. *Proc. Natl. Acad. Sci. USA* **97**, 7058–7063 (2000).
- Scanlan, T.S., Prudent, J.R. & Schultz, P.G. Antibody-catalyzed hydrolysis of phosphate monoesters. *J. Am. Chem. Soc.* **113**, 9397–9398 (1991).
- Wentworth, P. Jr. et al. A bait and switch hapten strategy generates catalytic antibodies for phosphodiester hydrolysis. *Proc. Natl. Acad. Sci. USA* **95**, 5971–5975 (1998).
- Wentworth, P. & Janda, K.D. Catalytic antibodies. *Curr. Opin. Chem. Biol.* **2**, 138–144 (1998).
- Spivak, D.A., Hoffman, T.Z., Moore, A.H., Taylor, M.J. & Janda, K.D. A comparison of flexible and constrained haptens in eliciting antibody catalysts for paraoxon hydrolysis. *Bioorg. Med. Chem.* **7**, 1145–1150 (1999).
- Stec, B., Hehir, M.J., Brennan, C., Nolte, M. & Kantrowitz, E.R. Kinetic and X-ray structural studies of three mutant *E. coli* alkaline phosphatases: insights into the catalytic mechanism without the nucleophile Ser102. *J. Mol. Biol.* **277**, 647–662 (1998).
- Coleman, J.E. Structure and mechanism of alkaline phosphatase. *Annu. Rev. Biophys. Biomol. Struct.* **21**, 441–483 (1992).
- Thatcher, G.R.J. & Kluger, R. Mechanism and catalysis of nucleophilic substitution in phosphate esters. *Adv. Phys. Org. Chem.* **25**, 99–265 (1989).
- Peracchi, A. Enzyme catalysis: removing chemically 'essential' residues by site-directed mutagenesis. *Trends Biochem. Sci.* **26**, 497–503 (2001).
- Davies, D.R., Padlan, E.A. & Sheriff, S. Antibody-antigen complexes. *Annu. Rev. Biochem.* **59**, 439–473 (1990).
- Zaccolo, M., Williams, D.M., Brown, D.M. & Gherardi, E. An approach to random mutagenesis of DNA using mixtures of triphosphate derivatives of nucleoside analogues. *J. Mol. Biol.* **255**, 589–603 (1996).
- Arnold, F.H. When blind is better: protein design by evolution. *Nat. Biotechnol.* **16**, 617–618 (1998).
- Chen, Y.L., Tang, T.Y. & Cheng, K.J. Directed evolution to produce an alkalophilic variant from a *Neocallimastix patriciarum* xylanase. *Can. J. Microbiol.* **47**, 1088–1094 (2001).
- Christians, F.C. & Loeb, L.A. Novel human DNA alkyltransferases obtained by random substitution and genetic selection in bacteria. *Proc. Natl. Acad. Sci. USA* **93**, 6124–6128 (1996).
- Martinez, M.A., Pezo, V., Marliere, P. & Wain-Hobson, S. Exploring the functional robustness of an enzyme by *in vitro* evolution. *EMBO J.* **15**, 1203–1210 (1995).
- Oue, S., Okamoto, A., Yano, T. & Kagamiyama, H. Redesigning the substrate specificity of an enzyme by cumulative effects of the mutations of non-active site residues. *J. Biol. Chem.* **274**, 2344–2349 (1999).
- Daugherty, P.S., Chen, G., Iverson, B.L. & Georgiou, G. Quantitative analysis of the effect of the mutation frequency on the affinity maturation of single chain Fv antibodies. *Proc. Natl. Acad. Sci. USA* **97**, 2029–2034 (2000).
- Takahashi, N., Kakinuma, H., Liu, L., Nishi, Y. & Fujii, I. *In vitro* abzyme evolution to optimize antibody recognition for catalysis. *Nat. Biotechnol.* **19**, 563–567 (2001).
- Ladner, R.C. & Ley, A.C. Novel frameworks as a source of high-affinity ligands. *Curr. Opin. Biotechnol.* **12**, 406–410 (2001).
- Jürgens, C., et al. Directed evolution of a ( $\beta\alpha$ )<sub>2</sub>-barrel enzyme to catalyze related reactions in two different metabolic pathways. *Proc. Natl. Acad. Sci. USA* **97**, 9925–9930 (2000).
- Hanes, J., Schaffitzel, C., Knappik, A. & Plückthun, A. Picomolar affinity antibodies from a fully synthetic naive library selected and evolved by ribosome display. *Nat. Biotechnol.* **18**, 1287–1292 (2000).
- Wolfenden, R., Ridgway, C. & Young, G. Spontaneous hydrolysis of ionized phosphate monoesters and diesters and the proficiencies of phosphohydrolases as catalysts. *J. Am. Chem. Soc.* **120**, 833–834 (1998).
- O'Brien, P.J. & Herschlag, D. Alkaline phosphatase revisited: hydrolysis of alkyl phosphates. *Biochemistry* **41**, 3207–3225 (2002).
- Honegger, A. & Plückthun, A. Yet another numbering scheme for immunoglobulin variable domains: an automatic modeling and analysis tool. *J. Mol. Biol.* **309**, 657–670 (2001).
- Kabat, E.A. & Wu, T.T. Identical V region amino acid sequences and segments of sequences in antibodies of different specificities. Relative contributions of VH and VL genes, minigenes, and complementarity-determining regions to binding of antibody-combining sites. *J. Immunol.* **147**, 1709–1719 (1991).